

New Anti-windup Structure for Magnitude and Rate Limited Inputs and Peak-Bounded Disturbances [★]

Maryam Sadeghi Reineh, Solmaz S. Kia, Faryar Jabbari

Department of Mechanical and Aerospace Engineering, University of California, Irvine

Abstract

A new structure for the anti-windup (AW) compensation for rate limited actuation is proposed which is less conservative than structures currently used. For peak bounded disturbances or reference inputs, we develop AW augmentation loops for both magnitude and rate actuator saturation. To reduce conservatism further, the proposed technique is combined with a multi-stage AW loops to obtain different gains for different levels of saturation.

Key words: anti-windup, magnitude and rate bounded actuators, multi-stage anti-windup loop, peak-to-peak gain.

1 Introduction

Input saturation due to limited capacity of actuators can cause significant performance degradation, even destabilization. In many applications, actuator can be saturated both in terms of the size and the rate of change of the signal. If saturation occurs occasionally (or episodically), a high performance nominal controller can still be used if some modifications, known as Anti-Windup (AW) compensation, are made. This will maintain the characteristics of the unconstrained system in small signal regimes and guarantee stability and improved performance once saturation nonlinearities are encountered.

As discussed in Galeani et al. [2008] and Reineh et al. [2016], the common energy-to-peak approach, in which the exogenous signal is assumed to be energy (norm) bounded, can be practically limiting. Here, in order to allow more realistic applications, unlike other references, the reference signals are assumed to be peak bounded and AW gains are achieved using the peak-to-peak approach (Boyd et al. [1994]) which could be seen as a variation of the traditional ultimate boundedness control.

For the peak-to-peak approach, the traditional AW structure is only feasible for large rate limits. In order to broaden the feasibility range when the rate limits are tight, and also to achieve higher performance, a new schematic of the Magnitude and Rate Anti-Windup (MRAW) is proposed in *Section. 3*. An alternative approach using dynamic AW loop has been proposed in

Sofrony et al. [2009]. As illustrated by the numerical results in *Section. 5*, compared to the traditional design, the new MRAW is feasible for much tighter saturation bounds and the guaranteed performance is also significantly better for both energy-to-peak and peak-to-peak approaches (Reineh et al. [2017]). Also, in this paper, to further reduce conservatism, the idea of multi-stage AW, first introduced in Kia and Jabbari [2011], is applied. This allows scheduling AW gains based on the saturation level, i.e., more aggressive AW gains, thus better performance, for moderately saturated signals.

2 Problem Statement

Let $0_{n \times m}$ be the n by m matrix of zeros and I_n the $n \times n$ identity matrix. For $A \in \mathbb{R}^{n \times m}$, A^\top is its transpose, while $A_{(i)}$ is its i th row. For a symmetric matrix A , $A > 0$ indicates that A is positive definite. Any matrix whose columns form bases of the null space of matrix A is denoted by \mathcal{N}_A , while, $\text{He}(A)$ is $A + A^\top$. Here, $x \mapsto y \in [0, I_n]$ denotes a decentralized nonlinear map, where $x_i \mapsto y_i$ belongs to sector $[0, 1]$ and $y_i^\top (x_i - y_i) \geq 0$ for all $x_i \in \mathbb{R}^n$ (Khalil [2002]). It is easy to see that if W is diagonal positive definite, then $y^\top W(x - y) \geq 0$ as well with $x = [x_1, \dots, x_n]^\top$ and $y = [y_1, \dots, y_n]^\top$.

Consider the linear plant P given by

$$\begin{aligned}\dot{x}_p &= A_p x_p + B_1 w + B_2 u_p, \\ z &= C_1 x_p + D_{11} w + D_{12} u_p, \\ y &= C_2 x_p + D_{21} w + D_{22} u_p,\end{aligned}\tag{1}$$

and the compensator C as

$$\begin{aligned}\dot{x}_c &= A_c x_c + B_{cy} y + B_{cw} w, \\ u &= C_c x_c + D_{cy} y + D_{cw} w.\end{aligned}\tag{2}$$

[★] Corresponding author: M. Sadeghi Reineh

Email address: {sadeghm1, solmaz, fjabbari}@uci.edu (Maryam Sadeghi Reineh, Solmaz S. Kia, Faryar Jabbari).

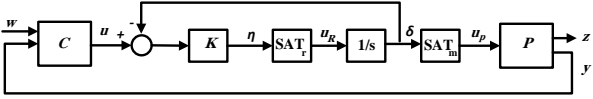


Fig. 1. The basic setup of the control loop.

We assume that actuators have magnitude and rate limits and commands sent to the actuators should not exceed these bounds; i.e., for every input, we require

$$|u_{pi}| \leq m_i, \quad |\dot{u}_{pi}| \leq r_i, \quad i \in \{1, \dots, n_u\}, \quad (3)$$

where r_i and m_i are known constants. We insert, via software, a first-order feedback loop containing two saturation elements between the controller and the plant, as shown in Fig. 1. The input to the plant u_p is thus

$$\dot{\delta} = \text{sat}_r(K(u - \delta)), \quad u_p = \text{sat}_m(\delta), \quad (4)$$

where $K = \text{diag}(K_1, \dots, K_{n_u}) \in \mathbb{R}_{>0}^{n_u \times n_u}$. The plant input signal u_p , is clearly magnitude bounded. Moreover, since its derivative is bounded due to the saturation before the integral block, the signal is rate bounded as well. The gain matrix K has to be chosen large enough such that it has minimal impact on nominal closed loop system. Compared to the design presented in Galeani et al. [2008], we do not require the access to the derivative of the compensator's output signal, thus, no need to neglect the effect of feed through and noise terms. Of course, in their set-up matrix K does not influence the dynamics when saturation is not faced and can be any positive definite diagonal matrix. The idea proposed here can be incorporated within that setup as well.

3 New MRAW Design: Peak-to-Peak Approach

Consider the block diagram in Fig. 2. Here, compared to the standard setup for MRAW, e.g. in Reineh et al. [2016], the key signal Γ , the first n_u elements of the magnitude and rate feedback signals, is added to the controller output. Signal Γ directly affects the rate dynamics and improves the performance, as discussed below.

In this paper, the MRAW design is conducted using peak-to-peak analysis with disturbance signals satisfying $w^\top w \leq w_{max}$ for some known w_{max} . Energy-to-peak (and \mathcal{L}_2 gain) results can be obtained with standard modifications thus are not repeated. The goal is to find the guaranteed peak for the closed-loop system performance output z for a peak bounded disturbance signal.

Assumption 1 (Nominal closed-loop system stable and no feed-through terms in performance output): The nom-

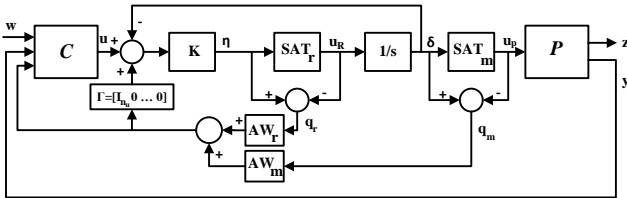


Fig. 2. New AW design for magnitude and rate saturation.

inal closed-loop system is required to be stable. The performance output is assumed to depend only on the states and have no feed-through terms; i.e., $z = C_1 x_p$. \square

Including the u term in performance output is straightforward but complicates the resulting LMIs, and inclusion of the w term requires an additional line search.

Assumption 2 (Peak bound on exogenous input): The exogenous input w , for some known $w_{max} \geq 0$, satisfies

$$w^\top(t)w(t) \leq w_{max}^2, \quad \forall t \geq 0. \quad (5)$$

Our objective is to obtain suitable additive signals $v_1 \in \mathbb{R}^{n_c}$ and $v_2 \in \mathbb{R}^{n_u}$ to the unconstrained controller (2), i.e., rendering the compensator as

$$\begin{aligned} \dot{x}_c &= A_c x_c + B_{cy} y + B_{cw} w + v_1, \\ u &= C_c x_c + D_{cy} y + D_{cw} w + v_2, \end{aligned} \quad (6)$$

such that the closed-loop system is internally stable with a guaranteed input-output performance measure χ .

For a given $w_{max} \in \mathbb{R}_{>0}$, we wish to minimize

$$z^\top(t)z(t) \leq \chi^2, \quad \text{for } w^\top(t)w(t) \leq w_{max}^2, \quad \forall t \geq 0. \quad (7)$$

For brevity, we combine the new design with Multi-stage structure introduced in Kia and Jabbari [2011]. For simplicity, we only show multiple stages on rate saturation.

3.1 Multi-Stage AW Design

To reduce the conservatism further, the multi-stage version of the new MRAW design is studied here. The main idea of the multi-stage AW is to schedule the gains based on the level of saturation to get a better performance when the signal is moderately saturated. As shown in Fig. 3, an additional saturation block, shown as ART. SAT, or artificial saturation, is added to the rate saturation element with bounds larger than the original saturation limits. The new block is responsible for bounding the sector nonlinearity of the original rate saturation block such that the corresponding deadzone q_r belongs to a smaller sector than $[0 \quad I]$. A larger limit of $\tilde{r} = \frac{r}{1-s_d}$, with $0 < s_d < 1$, is selected for the additional element which guarantees $|u_d| < \frac{r}{1-s_d}$. By setting $s_d = 0$, the second saturation element will never be activated, while with $s_d \approx 1$, the sector $q_r \in [0 \quad I]$ of the single-stage design is recovered. Therefore, by using $0 < s_d < 1$ the size of the rate deadzone sector is shrunk and more aggressive anti-windup gains may be triggered by q_r . The main idea is to have different anti-windup gains for when the rate command is high (triggered by \tilde{q}_r), than when it is modest ($\tilde{q}_r = 0$ but $q_r \neq 0$) which would result in more aggressive anti-windup gains. As shown in Fig. 3,

$$\tilde{q}_r = dz(\eta) = \eta - \text{sat}_R(\eta) = \eta - u_d, \quad (8)$$

$$q_r = dz(u_d) = u_d - \text{sat}_R(u_d) = u_d - u_R,$$

$$q_m = dz(\delta) = \delta - \text{sat}_M(\delta) = \delta - u_p.$$

We also have, $\eta = K(u - \delta + \Gamma)$, and

$$\Gamma = [I_{n_u} \quad 0_{n_u \times n_c}] (\Lambda_m q_m + \Lambda_r q_r + \tilde{\Lambda}_r \tilde{q}_r). \quad (9)$$

Therefore, $u_R = K(u - \delta + \Gamma) - q_r - \tilde{q}_r$. Since $\delta = \frac{1}{s} u_R$, the signal δ is a new state variable with dynamics

$$\dot{\delta} = K(u - \delta + \Gamma) - q_r - \tilde{q}_r, \quad (10)$$

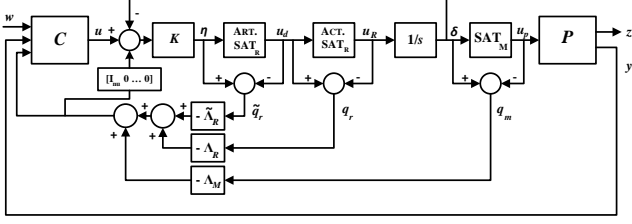


Fig. 3. Multi-stage AW for magnitude and rate saturation.

in which the signal u can be substituted from (2). Note that (10) shows that signal Γ enters the dynamics of the integrator directly. Moreover, $v_1 = -[I_{n_c} \ 0](\Lambda_m q_m + \Lambda_r q_r + \tilde{\Lambda}_r \tilde{q}_r)$ and $v_2 = -[0 \ I_{n_u}](\Lambda_m q_m + \Lambda_r q_r + \tilde{\Lambda}_r \tilde{q}_r)$. The closed loop system is then

$$\begin{aligned} \dot{x} &= Ax + B_w w + (B_{q_m} - B_\eta \Lambda_m) q_m + (B_{q_r} - B_\eta \Lambda_r) q_r \\ &\quad + (B_{q_r} - B_\eta \tilde{\Lambda}_r) \tilde{q}_r, \\ z &= C_z x, \\ u &= C_u x + D_{uw} w + (D_{uq} - D_{u\eta} \Lambda_m) q_m - D_{u\eta} \Lambda_r q_r \\ &\quad - D_{u\eta} \tilde{\Lambda}_r \tilde{q}_r, \end{aligned} \quad (11)$$

with system matrices given by

$$\begin{aligned} \left[\begin{array}{c|c} A & B_{q_m} \\ \hline C_z & D_{zq} \\ \hline C_u & D_{uq} \end{array} \right] &= \left[\begin{array}{ccc|c} A_p & 0 & B_2 & -B_2 \\ B_{cy} C_2 & A_c & B_{cy} D_{22} & -B_{cy} D_{22} \\ \hline K D_{cy} C_2 & K C_c & K(D_{cy} D_{22} - I) & -K D_{cy} D_{22} \\ \hline C_1 & 0 & D_{12} & -D_{12} \\ \hline D_{cy} C_2 & C_c & D_{cy} D_{22} & -D_{cy} D_{22} \end{array} \right] \\ \left[\begin{array}{c|c|c} B_w & B_\eta & B_{q_r} \\ \hline D_{uw} & D_{u\eta} & D_{zq} \end{array} \right] &= \left[\begin{array}{ccc|ccc} B_1 & 0 & 0 & 0 & 0 & 0 \\ B_{cy} D_{21} + B_{cw} & I & 0 & 0 & 0 & 0 \\ \hline K(D_{cy} D_{21} + D_{cw}) & K[I \ 0] & K & -I & & \\ \hline D_{cy} D_{21} + D_{cw} & 0 & I & D_{11} & & \end{array} \right]. \end{aligned}$$

Compared to the system matrices of the standard MRAW, only the B_η matrix has changed, having the gain K appearing in the last row block. As shown in the numerical examples in Section 5, this change improves the performance of the MRAW design significantly.

The key technical element here relies on the so-called slack variables (e.g. Lin [1998]). The following Lemma, based on Lemma 1 of da Silva and Tarbouriech [2005], identifies key properties of slack variables H_m and \tilde{H}_r .

Lemma 3 (Multi-stage AW sector conditions): Consider the polyhedral set S for $i = \{1, \dots, n_u\}$ defined as

$$S = \{x \in \mathbb{R}^n : |H_{m(i)} x| \leq m_i, |\tilde{H}_{r(i)} x| \leq \tilde{r}_i\}, \quad (12)$$

where matrices H_m and \tilde{H}_r are free parameters to be determined. Then, given the sector conditions

$$\begin{aligned} \delta &\mapsto q_m \in [0 \ I], \quad u_d \mapsto q_r \in [0 \ s_d I], \\ \eta &\mapsto \tilde{q}_r \in [0 \ I], \end{aligned} \quad (13)$$

for $x \in S$, the following inequalities hold

$$\begin{aligned} (a) \quad & q_m^\top W_m (q_m - \delta + H_m x) \leq 0, \\ (b) \quad & q_r^\top W_r (q_r - s_d u_d) \leq 0, \\ (c) \quad & \tilde{q}_r^\top \tilde{W}_r (\tilde{q}_r - \eta + \tilde{H}_r x) \leq 0, \end{aligned} \quad (14)$$

with diagonal positive definite matrices \tilde{W}_r , W_r and W_m .

PROOF. Similar to Reineh et al. [2016] \square

The following theorem employs the sector conditions introduced in Lemma 3 and establishes the optimization problem to obtain the AW gains in Fig. 3.

Theorem 4 (Multi-stage MRAW): Consider the plant (1), its nominal controller (2), and Assumptions 1 and 2. Given the bounds m and r on the actuator magnitude and rate, respectively, assume for a given $0 < \alpha < \frac{|\text{Re}(\lambda_{\min}(A))|}{2}$, there exists a solution for

$$\min_{Q, \bar{Q}, M_m, M_r, \tilde{M}_r, X_m, X_r, \tilde{X}_r, Y_m, \tilde{Y}_r, \chi^2, \tilde{\chi}^2} c_1 \chi^2 + c_2 \tilde{\chi}^2 \quad (15)$$

subject to

$$\begin{pmatrix} QA^\top + AQ + \alpha Q & * & * & * & * \\ B_w^\top & -\alpha I & * & * & * \\ \Phi_{3,1} & 0 & -2M_m & * & * \\ \Phi_{4,1} & K D_{uw} & \Phi_{4,3} & \Phi_{4,4} & * \\ \Phi_{5,1} & K D_{uw} & \Phi_{5,3} & \Phi_{5,4} & \Phi_{5,5} \end{pmatrix} < 0, \quad (16)$$

$$\begin{pmatrix} \bar{Q}A^\top + A\bar{Q} + \alpha\bar{Q} & * & * & * \\ B_w^\top & -\alpha I & * & * \\ \bar{\Phi}_{3,1} & 0 & -2M_m & * \\ \bar{\Phi}_{4,1} & K D_{uw} & \Phi_{4,3} & \Phi_{4,4} \end{pmatrix} < 0, \quad (17)$$

$$\begin{pmatrix} Q & QC_z^\top \\ C_z Q & \chi^2/w_{max}^2 \end{pmatrix} > 0, \quad \begin{pmatrix} \bar{Q} & \bar{Q}C_z^\top \\ C_z \bar{Q} & \tilde{\chi}^2/w_{max}^2 \end{pmatrix} > 0, \quad (18)$$

$$\begin{pmatrix} m_i^2/w_{max}^2 & Y_{mi} \\ Y_{mi}^\top & Q \end{pmatrix} > 0, \quad \begin{pmatrix} r_i^2/w_{max}^2 & \tilde{Y}_{ri} \\ \tilde{Y}_{ri}^\top & Q \end{pmatrix} > 0, \quad (19)$$

$$\begin{pmatrix} m_i^2/w_{max}^2 & \tilde{Y}_{mi} \\ \tilde{Y}_{mi}^\top & \bar{Q} \end{pmatrix} > 0. \quad (20)$$

where $i = 1, \dots, n_u$, $\tilde{r} = \frac{r}{1-s_d}$, and

$$M_m = W_m^{-1}, \quad M_r = (W_r s_d)^{-1}, \quad \tilde{M}_r = \tilde{W}_r^{-1}, \quad (21)$$

$$X_m = \Lambda_m M_m, \quad X_r = \Lambda_r M_r, \quad \tilde{X}_r = \tilde{\Lambda}_r \tilde{M}_r,$$

$$\Phi_{3,1} = M_m B_{q_m}^\top - X_m^\top B_\eta^\top + [0 \ 0 \ I] Q - Y_m,$$

$$\Phi_{4,1} = M_r B_{q_r}^\top - X_r^\top B_\eta^\top + [C_u - [0 \ 0 \ I]] K Q,$$

$$\Phi_{5,1} = \tilde{M}_r B_{q_r}^\top - \tilde{X}_r^\top B_\eta^\top + [C_u - [0 \ 0 \ I]] K Q - \tilde{Y}_r,$$

$$\Phi_{4,3} = K D_{uq} M_m - K D_{u\eta} X_m + s_d K [1 \ 0] X_m,$$

$$\Phi_{4,4} = -2M_r s_d^{-1} - \text{He}(K D_{u\eta} X_r - s_d K [1 \ 0] X_r),$$

$$\Phi_{5,3} = K D_{uq} M_m - K D_{u\eta} X_m + K [1 \ 0] X_m, \quad (22)$$

$$\Phi_{5,4} = -\tilde{M}_r - K D_{u\eta} X_r - K \tilde{X}_r^\top D_{u\eta}^\top$$

$$+ K [1 \ 0] X_r + s_d K \tilde{X}_r^\top [1 \ 0]^\top,$$

$$\Phi_{5,5} = -2\tilde{M}_r - \text{He}(K D_{u\eta} \tilde{X}_r - K [1 \ 0] \tilde{X}_r),$$

$$\bar{\Phi}_{3,1} = M_m B_{q_m}^\top - X_m^\top B_\eta^\top + [0 \ 0 \ I] \bar{Q} - \tilde{Y}_m,$$

$$\bar{\Phi}_{4,1} = M_r B_{q_r}^\top - X_r^\top B_\eta^\top + [C_u - [0 \ 0 \ I]] K \bar{Q},$$

with $Y_m = H_m Q$, $\tilde{Y}_r = \tilde{H}_r Q$, $\bar{Y}_m = H_m \bar{Q}$.

Then the closed loop system (11), has reachable set

$$x(t) \in \mathcal{E}(Q^{-1}, w_{max}^2) = \{x : x^\top Q^{-1} x < w_{max}^2\}, \quad (23)$$

and performance level gain χ from w to z , $z^\top(t)z(t) \leq \chi^2$, as long as the disturbance signals satisfy $w^\top(t)w(t) \leq w_{max}^2$ and $x(0) = 0$. Moreover, for moderate levels of saturation specified as $|\eta| \leq \tilde{r} = \frac{r}{1-s_d}$, $\bar{\chi} < \chi$ is the upper bound for the performance level.

Proof. Satisfaction of (19) implies that the set (23) is included in the polyhedral set (12) (Boyd et al. [1994]). Inequality (16) is equivalent to

$$\begin{aligned} & \frac{d}{dt}(x^\top Q^{-1}x) + \alpha x^\top Q^{-1}x - \alpha w^\top w \\ & - 2q_m^\top W_m(q_m - \delta + H_m x) - 2q_r^\top W_r(q_r - s_d u_d) \\ & - 2\tilde{q}_r^\top W_r(\tilde{q}_r - \eta + \tilde{H}_r x) < 0. \end{aligned} \quad (24)$$

Invoking Lemma 3, (24) reduces to $\dot{V} + \alpha(V - w^\top w) < 0$, with Lyapunov function $V = x^\top Q^{-1}x$ and $Q > 0$, as a result, (23) is established as the invariant set. Thus, (19) establishes upper bounds for Euclidean norm of H_m and \tilde{H}_r over the invariant ellipsoid established by (16)-(20), with performance level χ guaranteed by (18).

For moderate levels of saturation specified as $|\eta| < \tilde{r} = \frac{r}{1-s_d}$, the sector condition $u_d \mapsto q_r \in [0 \ s_d I]$ is in effect and according to Lemma 3, the inequality $q_r^\top W_r(q_r - s_d u_d) \leq 0$ will be satisfied. Using the Lyapunov function $V = x^\top Q^{-1}x$, the inequality (17), gives

$$\frac{d}{dt}(x^\top \bar{Q}^{-1}x) + \alpha x^\top Q^{-1}x - \alpha w^\top w < 0, \quad (25)$$

and (18) (right) establishes performance $\bar{\chi}$, if the artificial saturation element is not activated. In this case, (20) plays the role of (19) (left). \square

Remark 5 Inequalities (16) and (18) (left) ensure that the closed-loop system is stable with gain χ , while (17) indicates gain $\bar{\chi}$ in case of a command with rate of change below $\tilde{r} = \frac{r}{1-s_d}$. For moderate saturation cases, larger values for c_2 can be used in order to achieve lower values for $\bar{\chi}$ and thus, more aggressive AW gains. This is at the cost of a larger χ , which is the guaranteed gain for the closed-loop, for arbitrary level of rate saturation. Here, $\bar{\chi}$ is a measure of the aggressiveness of AW gains.

Remark 6 In Theorem 4, α enters the inequality in a product form. For optimized performance, a line search is done, as in other peak-to-peak gain problems. Energy-to-peak approach does not have the line search but gives considerably more conservative results.

4 Feasibility Analysis

In this section we show that the feasibility of the multi-stage design (Theorem 4) is the same as the feasibility of the single-stage design. Note that with $\bar{Q} = Q$ and $\bar{\chi} = \chi$, inequalities (18) and (20) are equivalent, and inequality (17) is the (1:4,1:4) block of (16). As a result, if (16) is feasible, then there exists at least one set of decision variables that make (17) and (20) feasible. In fact,

the presence of \bar{Q} , $\bar{\chi}$, increases the degrees of freedom and allows for a better performance. Therefore, here we only study the feasibility of inequality (16).

Lemma 7 The matrix inequality presented in (16) is feasible if and only if

$$\begin{pmatrix} QA^\top + AQ + \alpha Q & * \\ B_w^\top & -\alpha I \end{pmatrix} < 0, \quad (26)$$

$$R < 0 \quad \text{and} \quad R - NM^{-1}N^\top < 0.$$

in which $M = -2M_r s_d^{-1}$, and

$$N = \begin{pmatrix} -\sum_{i=1}^3 \tilde{H}_{ri} Q_{1i}^\top & 0 & 0 & \sum_{i=1}^3 \tilde{H}_{ri} Q_{i3} \end{pmatrix}^\top \quad (27)$$

$$R = \begin{pmatrix} He(A_p Q_{11} + B_2 Q_{13}^\top) + Q_{11} \alpha & * & * & * \\ B_1^\top & -\alpha I & * & * \\ C_1 Q_{11} + D_{12} Q_{13}^\top & 0 & -2M_m & * \\ -\sum_{i=1}^3 \tilde{H}_{ri} Q_{1i}^\top + Q_{13}^\top \alpha & 0 & R_{43} & R_{44} \end{pmatrix},$$

$$R_{43} = -Q_{33} + \left(\sum_{i=1}^3 H_{mi} Q_{i3}\right)^\top,$$

$$R_{44} = He\left(\sum_{i=1}^3 \tilde{H}_{ri} Q_{i3}\right)^\top + Q_{33} \alpha.$$

Proof. Inequality (16) can be represented as

$$\Psi + He\{G^\top [\tilde{X}_r \ X_r \ X_m] H\} < 0, \quad (28)$$

where Ψ is (16) without the X_m , X_r , \tilde{X}_r terms, and

$$G = \begin{pmatrix} 0 & 0 & 0 & 0 & I \\ 0 & 0 & 0 & I & 0 \\ 0 & 0 & I & 0 & 0 \end{pmatrix}^\top, \quad \mathcal{N}_G = \begin{pmatrix} I & 0 & 0 & 0 & 0 \\ 0 & I & 0 & 0 & 0 \end{pmatrix}^\top, \quad (29)$$

and $H = \begin{pmatrix} -B_\eta^\top & 0 & 0 & -D_{u\eta}^\top K & -D_{u\eta}^\top K \end{pmatrix}$. Recalling elimination lemma from Boyd et al. [1994], (28) is feasible if and only if $\mathcal{N}_G^\top \Psi \mathcal{N}_G < 0$ and $\mathcal{N}_H^\top \Psi \mathcal{N}_H < 0$. Substituting from (29), the first condition results in (26). Partition Q as $Q = [Q_{ij}]$ with $i, j = \{1, 2, 3\}$. The second condition $\mathcal{N}_H^\top \Psi \mathcal{N}_H < 0$ after a row-column manipulations can be expressed as

$$\mathcal{N}_H^\top \Psi \mathcal{N}_H = \left(\begin{array}{c|c} R & N \\ \hline N^\top & M \end{array} \right) < 0, \quad (30)$$

with R , and N given in (27). By Schur complement, (30) is equivalent to $R - NM^{-1}N^\top < 0$. \square

For the single-stage design, the additional saturation block is removed, thus, we do not have s_d anymore. Following the proof of Lemma 7, for the single-stage design, \mathcal{N}_G and \mathcal{N}_H are the same as the multi-stage design after removing their last row and column. Thus, the single-stage design is feasible if and only if (26) and $\bar{R} < 0$, where \bar{R} is equivalent to R in (26), except for \tilde{H}_r which is replaced by H_r .

According to (26), since the free variable M_r only appears in matrix M , it is possible to make the second term

in $R + NM^{-1}N^T < 0$ arbitrary small, by choosing M_r to be large enough. Thus, the feasibility condition for the multi-stage design reduces to the feasibility condition of the single-stage design.

5 Simulation Results

In this section, we evaluate the performance of the proposed MRAW using the peak-to-peak approach. For simplicity, a SISO example is presented here, although the proposed techniques has been evaluated on MIMO systems as well. For \mathcal{L}_2 gain results, see Reineh et al. [2017].

Consider the example from Dorf and Bishop [2008], for an aircraft pitch dynamics with the unconstrained system block diagram shown in Fig. 4. The aircraft transfer function $G_p(s)$ with the pitch rate, $\dot{\theta}$, as output, and the elevator deflection, δ , as input, is given by

$$G_p(s) = \frac{\dot{\theta}(s)}{\delta(s)} = \frac{-10(s+1)(s+0.01)}{(s^2+2s+2)(s^2+0.02s+0.0101)}.$$

Next, a fourth-order state-space representation is obtained. The performance output is then taken to be $z = y - w$. In Dorf and Bishop [2008], the lead compensator $G_c(s) = -4\frac{s+2}{s+22}$ is designed for the unconstrained system that meets the desired specifications.

Using the peak-to-peak method, the lowest rate limit for which the standard design, i.e. without Γ , is feasible is $r = 68$. While the new design is feasible for much lower saturation bounds and the AW gains achieved are capable of improving the performance significantly. In this example, the limits for the input magnitude and rate are selected as $m = 6$ and $r = 10$, respectively, with $w_{max} = 1$ and $K = 10$. The peak-to-peak design without signal Γ is not feasible for these tight bounds.

For the multi-stage design with $s_d = 0.2$, $c_1 = 1$ and $c_2 = 10$, the static gains $\Lambda_m = [-0.3425 \ 0.8710]^T$, $\Lambda_r = [-0.0140 \ -0.0344]^T$, and $\tilde{\Lambda}_r = [-0.0651 \ 0.2106]^T$ are achieved with a guaranteed regional performance level of $\chi = 8.7359$. Moreover, assuming low to moderate rate saturation, a better performance measure of $\bar{\chi} = 6.7404$ can be achieved through a more aggressive AW design. The single-stage magnitude and rate anti-windup compensation results in $\chi = 7.701$ with $\Lambda_m = [-0.4664 \ 1.4056]^T$, $\Lambda_r = [-0.0258 \ 0.0201]^T$. The response of the system to a reference signal satisfying $w^T w \leq 1$ is shown in Fig. 5 using the multi-stage and the single-stage magnitude and rate AW designs. Both of the techniques have improved the performance of the saturated system significantly, however, the multi-stage design provides a closer performance to the response of the unconstrained system.

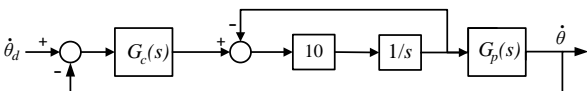


Fig. 4. An aircraft pitch rate feedback control system.

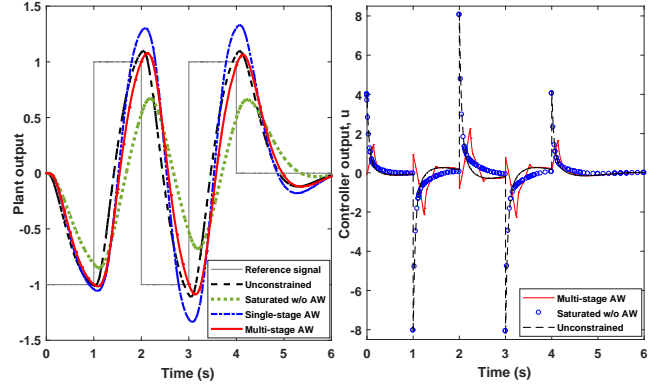


Fig. 5. Performance of the multi-stage MRAW with $r = 6$, $m = 10$, $s_d = 0.2$, $\alpha = 0.03$.

6 Conclusions

We presented a novel structure for MRAW design (single and multi-stage) accommodating peak bounded exogenous signals. The new structure and the peak-to-peak analysis applied provide compensation for more practical problems with tighter rate bounds which could not be solved using the traditional AW structures.

References

- Boyd, S., Ghaoui, L. E., Feron, E. and Balakrishnan, V. [1994], *Linear Matrix Inequalities in System and Control Theory*, 1st edn, SIAM, Philadelphia, PA.
- da Silva, J. M. G. and Tarbouriech, S. [2005], ‘Anti-windup design with guaranteed regions of stability: An lmi-based approach’, *IEEE Transactions on Automatic Control* **50**(1), 106–111.
- Dorf, R. C. and Bishop, R. H. [2008], *Modern Control Systems*, 11th edn, Prentice Hall, NJ.
- Galeani, S., Onori, S., Teel, A. R. and Zaccarian, L. [2008], ‘A magnitude and rate saturation model and its use in the solution of a static anti-windup problem’, *Systems and Control Letters* **57**(1), 1–9.
- Khalil, H. K. [2002], *Nonlinear Systems*, 3rd edn, Prentice Hall, NJ.
- Kia, S. S. and Jabbari, F. [2011], ‘Multi-stage anti-windup compensation for open loop stable plants’, *IEEE Transactions on Automatic Control* **56**(9), 2166–2172.
- Lin, Z. [1998], ‘Semi-global stabilization of discrete-time linear systems with position and rate-limited actuators’, *Systems and Control Letters* **34**(5), 313–322.
- Reineh, M. S., Kia, S. and Jabbari, F. [2016], Multi-stage anti-windup for LTI systems with actuator magnitude and rate saturation, in ‘American Control Conference’, Boston, MA, pp. 5455–5460.
- Reineh, M. S., Kia, S. and Jabbari, F. [2017], Anti-windup designs for systems with magnitude and rate bound actuators, in ‘IFAC World Congress’, Toulouse, France, pp. 11509–11514.
- Sofrony, J., Turner, M. C. and Postlethwaite, I. [2009], A simple anti-windup compensation scheme for systems with rate-limited actuators, in ‘ICCAS-SICE Int. Joint Conf.’, Fukuoka, Japan, pp. 3311–3316.